

Poly(ethylene glycol) Self-Assembled Monolayer Island Growth

Jonas Rundqvist,[†] Jan H. Hoh,[‡] and David B. Haviland^{*,†}

Nanostructure Physics, AlbaNova University Center, Royal Institute of Technology, Roslagsvägen 30 B, SE-106 91 Stockholm, Sweden, and Department of Physiology, Johns Hopkins School of Medicine, 725 North Wolfe Street, Baltimore, Maryland 21205

Received November 16, 2004. In Final Form: January 3, 2005

Here, we report a study of the morphology and growth dynamics of a self-assembled monolayer (SAM) of the amide containing poly(ethylene glycol) (PEG) thiol ($\text{CH}_3\text{O}(\text{CH}_2\text{CH}_2\text{O})_{17}\text{NHCO}(\text{CH}_2)_2\text{SH}$) on atomically flat Au(111) surfaces. SAM growth from a 20 μM ethanolic solution reveals island growth through three distinct steps: island nucleation, island growth, and coalescence. The coalescence-step, filling voids in the SAM, is by far slowest. The fine structure study reveals dendritic island formation, an observation which can be explained by attractive intermolecular interactions and surface diffusion-limited aggregation. We have also observed a change in the island height, which peaks during the island growth phase. This height change can be associated with a molecular conformational transition.

Introduction

Poly(ethylene glycol) (PEG)¹ molecules have been used extensively as a biocompatible material because of their low toxicity, low immunogenicity, and the ability to prevent nonspecific protein adsorption and cell adhesion.² Surfaces modified with self-assembled monolayers (SAMs) of oligo-(ethylene glycol) (OEG) or PEG can have excellent protein and cell repelling properties.^{3–5} We have a long-term interest in developing methods for nanometer scale patterning of functional biomolecules on surfaces; as part of this effort, we have been exploring the use of PEG as a component of such surfaces. Producing high-quality SAMs requires an understanding of how the monolayers are formed and organized; this has prompted us to study in some detail the behavior of the PEG thiol system.

Several attachment chemistries have been developed to functionalize surfaces with PEG, including SAM formation from thiolated PEGs onto Au and Ag,^{6–10} as well as through silane chemistry on SiO_2 ^{11,12} and glass

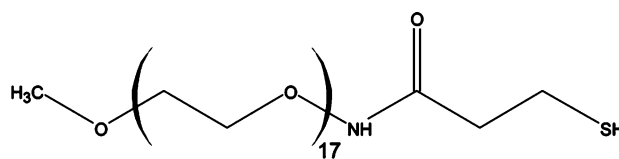


Figure 1. Chemical structure of the PEG thiol (MW 750 Da) used in this study. A thiol headgroup is linked with an alkane diol and an amide group to 17 units of ethylene glycol, terminating with a methyl group. All of these parts of the molecule could significantly contribute to the dynamics and structure of the SAM: the thiol by covalent binding to the Au atoms of the surface, the amide through lateral intramolecular hydrogen bonds and the ethylene glycol through both intra- and intermolecular interactions. PEG is a hydrophilic molecule which does not spontaneously form aggregates in either aqueous or ethanolic solutions.

surfaces.¹³ SAM formation from PEG thiolates typically involves an alkane thiol with a terminal PEG group of varying length. A great deal is known about alkane thiol SAMs, both with and without PEG extensions. The monolayer assembly of PEG-terminated alkane thiols is thought to be driven by lateral association of the alkane chains, resulting in a well-ordered SAM close to the surface with functional PEG at the terminus. During the growth process of alkane thiol SAMs with characteristic island growth, the individual alkane chains are organized from an initial low-order state of molecules laying down on the surface to a well-ordered crystalline state where the chains are densely packed and aligned at $\sim 30^\circ$ toward the surface normal to optimize the intermolecular van der Waals contact. There is a general consensus in the literature that this assembly is driven by lateral interactions between the alkane chains.¹⁴ In the cases with a PEG terminal group on an alkane thiol, there are several conformations of the PEG, including a disordered “molten” phase and a well-ordered phase with an all-trans and a 7/2 helical conformation.^{6–10} However, the PEG moiety has not been assigned any special role in promoting SAM formation.

In this paper, we examine the self-assembly of the amide-containing PEG thiol $\text{CH}_3\text{O}(\text{CH}_2\text{O})_{17}\text{NHCO}(\text{CH}_2)_2\text{SH}$ (Figure 1). In contrast to alkane-containing PEGs,

* To whom correspondence should be addressed. Telephone: +46 (0)8 5537 8137; fax: +46 (0)8 5537 8466; e-mail: haviland@nanophys.kth.se.

[†] Royal Institute of Technology.

[‡] Johns Hopkins School of Medicine.

(1) PEG is also referred to as poly(ethylene oxide) (POE) or poly(oxyethylene) (POE). The term PEG is commonly used for molecules with less than 150 ethylene glycol (EG) subunits. In this paper, the $\text{CH}_3\text{O}(\text{CH}_2\text{O})_{17}\text{NHCO}(\text{CH}_2)_2\text{SH}$ molecule will be denoted PEG thiol or PEG.

(2) Golander, C. G.; Herron, J. N.; Kim, J. N.; Claesson, P.; Stenius, P.; Andrade, J. D. *Poly(ethylene glycol) chemistry: Biotechnology and biomedical applications*; Harris, J. M., Ed.; Plenum Press: New York, 1992.

(3) Prime, K. L.; Whitesides, G. *Science* **1991**, *252*, 1164–1167.

(4) Desai, N. P.; Hubbell, J. A. *Biomaterials* **1991**, *12*, 144–153 and references therein.

(5) Lee, J. H.; Kopecek, J.; Andrade, J. D. *J. Biomed. Mater. Res.* **1989**, *23*, 351–368.

(6) Vanderah, D. J.; Pham, P. P.; Springer, S. K.; Silin, V.; Meuse, C. W. *Langmuir* **2000**, *16*, 6527–6532.

(7) Zolk, M.; Eisert, F.; Pipper, J.; Herrenwerth, S.; Eck, W.; Buck, M.; Grunze, M. *Langmuir* **2000**, *16*, 5849–5852.

(8) Valiokas, R.; Svedhem, S.; Svensson, S. C. T.; Liedberg, B. *Langmuir* **1999**, *15*, 3390–3394.

(9) Harder, P.; Grunze, M.; Dahnit, G. M.; Whitesides, G. M.; Laibnis, P. E. *J. Phys. Chem. B* **1998**, *102*, 426–436.

(10) Vanderah, D. J.; Meuse, C. W.; Silin, V.; Pland, A. L. *Langmuir* **1998**, *14*, 6916–6923.

(11) Sharma, S.; Johnson, R. W.; Desai, T. A. *Appl. Surf. Sci.* **2003**, *206*, 218–229.

(12) Sanderson, L. A. W.; Emoto, K.; van Alstine, J. M.; Weimer, J. *J. Colloid Interface Sci.* **1998**, *207*, 180–183.

(13) Jo, S.; Park, K. *Biomaterials* **2000**, *21*, 605–616.

(14) (a) Schreiber, F. *Prog. Surf. Sci.* **2000**, *65*, 151–256. (b) Schwartz, D. K. *Annu. Rev. Phys. Chem.* **2001**, *52*, 107–137. These reviews cover structure and growth as well as mechanisms and kinetics of SAM formation.

little is known about the structure and growth dynamics of SAMs with this class of molecule. In our experiments, the PEG thiol was allowed to adsorb onto flame-annealed Au surfaces for increasing lengths of times (1 min to several days). Organization of the monolayer was followed in a time-lapse fashion, using atomic force microscopy (AFM). AFM is a particularly useful tool for this type of study and has been used to examine PEG molecules on a variety of surfaces, such as grafted on porous polyurethanes polymer membrane¹⁵ and as a SAM on SiO₂, both dry¹¹ and in solution.^{12,13} We find that the PEG SAM, like alkane thiol SAMs, grows by island formation. However, the morphology of the islands is significantly different for the PEG thiol compared with alkane thiol islands. The island growth of the PEG is a notable finding, because there is no dominant alkane part in these molecules to provide the attractive interactions which are necessary for island formation. In particular, our PEG thiol shows dendritic islands, with a branching structure and many voids, suggesting aggregation through surface diffusion. We have also observed variations in height for the PEG islands during the island growth phase, which may be related to different conformations for the PEG.

This AFM study complements previous studies of PEG SAMs, providing detailed data on morphology and growth dynamics and adding to the ongoing discussion about the nature and applications of PEG SAMs.

Experimental Details

Preparation of Au Surfaces. $7 \times 5 \text{ mm}^2$ chips are cut out of a $250\text{-}\mu\text{m}$ -thick silicon wafer with $1\text{-}\mu\text{m}$ -thick SiO₂ surface layer. An array of $20 \times 20 \mu\text{m}^2$ Au films was made with a standard lift-off lithography process, and an e-beam system (Turnkey 150, Raith GmbH, Dortmund, Germany) was used to write the pattern in a double-layer e-beam resist. (Details of lift-off lithography process can be found elsewhere.)¹⁶ A Ti sticking layer (20 \AA thick) was deposited prior to the Au evaporation. The Au films as deposited in an e-gun evaporation system (base pressure 2×10^{-9} Torr) are very granular, and flame annealing was used to reconstruct the surface. In our experience, flame annealing is improved when using $20 \times 20 \mu\text{m}^2$ Au films rather than a completely covered surface since overheating is avoided. Flame annealing was performed with a simple setup where the chips with the Au squares were held with a pair of tweezers fixated on a stage. A hydrogen flame was swept back and forth at approximately 2 Hz frequency over the chip. Twelve minutes was a sufficient time, and longer anneal times showed no improvement in surface structure (Figure 2). The sweeping motion prevented overheating of the surface (orange glow from the chip). After flame annealing, the chip is allowed to cool for a minute in room temperature.

Chip Cleaning. The chips and tweezers used for handling the chips were immersed into a TL1 washing solution (H₂O₂/NH₃/H₂O 5:1:1, v/v) and heated to 50 °C for 10 min to remove organic contamination. The chips were then carefully rinsed with large quantities of MilliQ deionized water ($>18 \text{ M}\Omega\text{cm}$) and bathed in ethanol before immersion in the PEG solution. Care was taken to keep the surface of the chips covered with solution when being transferred between different solutions.

Preparation of PEG SAMs on Au. The PEG molecules (CH₃O(CH₂CH₂O)₁₇NHCO(CH₂)₂SH) were purchased from Rapp Polymere GmbH (Tübingen, Germany). The chips with the flame-annealed Au surfaces were lowered into 25 mL of $20 \mu\text{M}$ ethanolic PEG thiol solution freshly prepared from stock solution. Immersion times in PEG solution were varied from 1 min to several days. After PEG treatment, chips were immersed in ethanol and

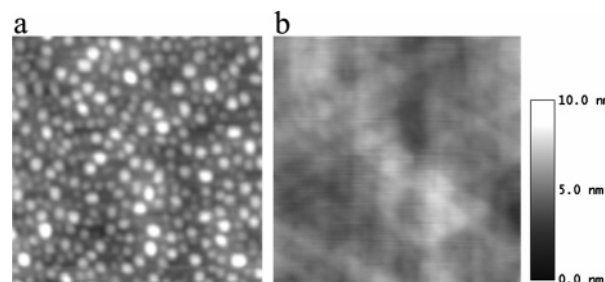


Figure 2. AFM images of evaporated Au surfaces (a) before and (b) after 12 min of flame annealing. Image sizes are $750 \times 750 \text{ nm}^2$. Thermal evaporation of Au using an e-gun source onto SiO₂ results in a granular Au surface with 20–40 nm grains, and imaging a PEG SAM on this surface reveals no useful structural information. The flame annealing increased the Au grain size to flat areas of several micrometers across, with less than 2-nm variation over $2 \mu\text{m}$. The resulting large crystalline area exhibited $60^\circ/120^\circ$, typical for good Au(111) surfaces. The annealed surfaces also displayed well-defined and clearly distinguishable terrace steps. The boundaries of the flat areas are separated by deep crevasses (Figure 3).

treated with ultrasound for 3 min to stop monolayer formation and to remove any PEG molecules not firmly attached to the surface. The chip surfaces were imaged directly after immersion and kept wet at all times.

Contact Mode AFM Studies in Fluid. The atomic force microscope used in this experiment was a commercially available MultiMode system with a J-scanner and a fluid cell, using the NanoScope IV controller (Veeco Metrology Group, Santa Barbara, CA). The data were collected using oxide-sharpened silicon nitride probes (Olympus OTR4 purchased from Veeco Metrology Group, Santa Barbara, CA) with a spring constant 0.08 N/m as calculated from the nominal cantilever dimensions and material properties. The samples were imaged with contact mode AFM in phosphate-buffered saline (PBS) with pH 7.4. We preferred to use contact mode AFM rather than tapping mode AFM. We have noticed a better resolution with contact mode. However, we have not seen any difference in monolayer height or any interference with the probe tip on the surface when comparing tapping mode and contact mode AFM in liquid. We believe that the SAM is a rather rigid formation and that eventual deformation of the SAM is comparable between the two techniques. The samples were imaged with a tip force of $\sim 0.1 \text{ nN}$, as calculated from the nominal spring constant and the cantilever deflection signal which was calibrated against the z -scanner displacement. The cantilever was allowed to find its thermal equilibrium, which took about 30 min after contact with the PBS at room temperature. The raw data was processed with NanoScope IV software by third-order plane-fit and first-order flattening.

Calculation of Surface Coverage and Island Height vs Immersion Time. By direct observation with AFM at different stages of SAM growth, quantitative information about the kinetics can be obtained. The high resolution in the z -axis allows us to unambiguously choose a threshold value of height for the separation of island coverage from the background of molecules laying on the surface. The threshold is determined from the histogram of height distribution using WSxM SPM software (Nanotec Electronica S.L.). Island coverage measurements were done by averaging at least four separate areas, each one no smaller than $\sim 700 \times 700 \text{ nm}^2$. The island height is extracted through a section analysis using the NanoScope IV software. The island height is defined as the distance from a lower pit of the PEG laying down close to a PEG island to the flat plateau of the PEG island. Island height measurements were made by averaging over at least 12 separate step heights on different sites.

Results

Monolayers were formed by immersion of the Au surfaces into an ethanolic PEG thiol solution, and subsequent characterization in the AFM was carried out in either ethanol or phosphate-buffered saline. Because

(15) Qiu, Y. X.; Klee, D.; Pluster, W.; Severich, B.; Höcker, H. *J. Appl. Polym. Sci.* **1996**, *61*, 2373–2382.

(16) Rundqvist, J. Investigations of Directed Protein Immobilization to Nano-Patterns Manufactured with E-Beam Lithography. Ph. Lic. Thesis, Royal Institute of Technology, Stockholm, Sweden, 2003; available at www.nanophys.kth.se.

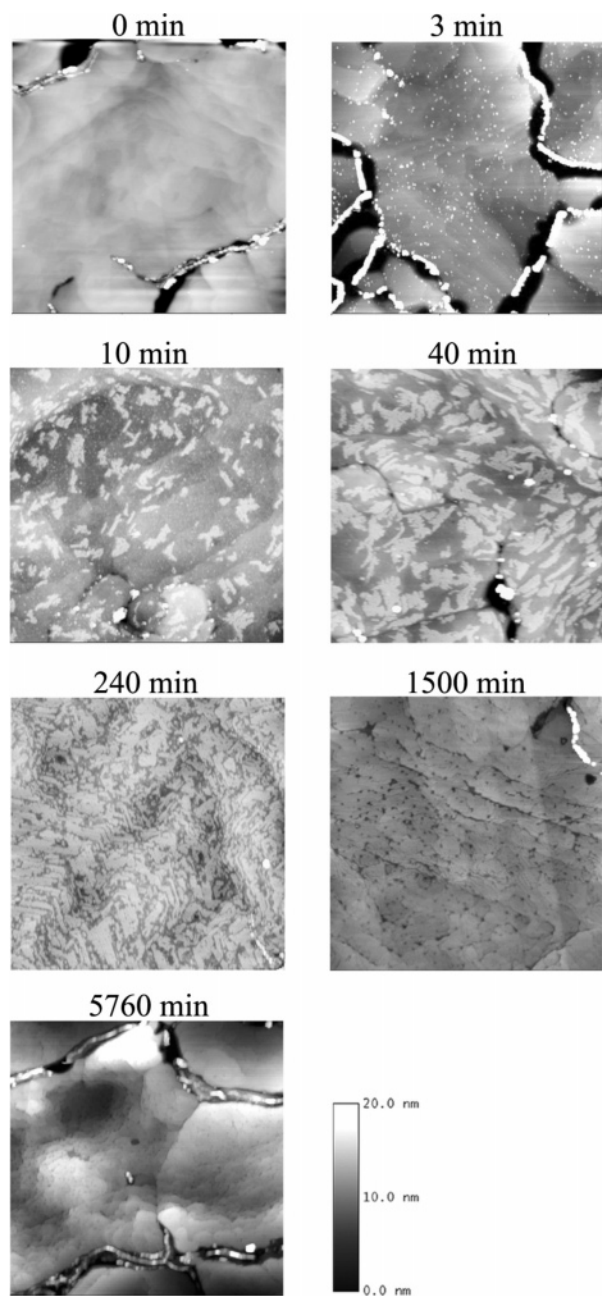


Figure 3. SAM growth of PEG thiol on flame-annealed Au from an ethanolic solution imaged in PBS with $2.5 \times 2.5 \mu\text{m}^2$ scans using contact mode AFM. The time elapsed since immersion of the chip into the PEG solution is given for each image. At 0 min (before immersion), the Au surface is clean. The nucleation phase (0–10 min), where the PEG molecules form an increasing number of small islands, is followed by an island growth phase (10–40 min). The coalescence of islands is observed after 240 min which proceeds very slowly toward a complete coverage of PEG.

our long-term interests are related to patterning surfaces with biomolecules, the majority of the characterization was performed in PBS. We present the PBS based characterization first and later compare the PBS results with ethanol.

The substrate of flame-annealed Au was essential to the use of AFM for SAM growth study. Obtaining a good AFM image of a SAM requires a flat substrate, with height variations significantly less than the SAM thickness. Au surfaces as evaporated typically consist of a densely packed film of Au grains with size 20–40 nm (Figure 2a). Flame annealing reconstructed the granular Au surface creating

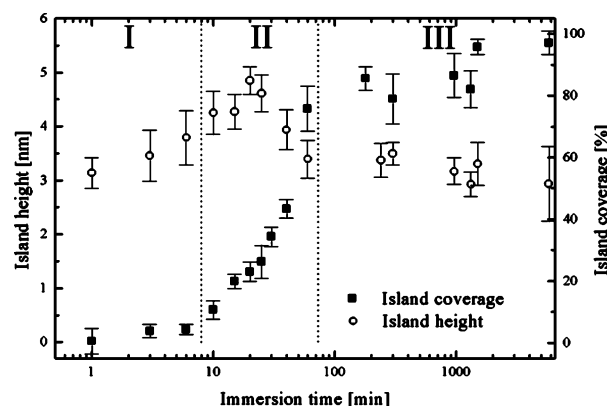


Figure 4. This semilog plot shows the PEG island coverage (solid points, right scale) and the variation of the PEG island thickness (open points, left scale) versus immersion time. Island coverage data was obtained by averaging the measurements over at least four separate areas, each one no smaller than $\sim 700 \times 700 \text{ nm}^2$. The island coverage shows a three-step growth behavior (separated with the dotted lines for clarity). The growth stages are characterized by island nucleation (I), island growth (II), and coalescence (III). There is a change in island height, which peaks during the island growth stage and levels out as the immersion time increases. Island height is determined through section analysis as shown in Figure 5. Island height measurements were made by averaging over ≥ 12 separate step heights on different sites. All error bars are standard deviations from measurements of island height and island coverage.

areas as large as $4 \mu\text{m}^2$ where the Au was single crystal, with height variations much less than the island height of the SAM (Figure 2b). Although the AFM cannot resolve individual atomic terraces (we have resolved these with STM), their presence on the surface causes the AFM image to display the sixfold symmetry of the Au(111) surface. These Au crystallites are separated by deep crevasses, visible in some of the images of Figure 3.

Time-lapse series of $2.5 \times 2.5 \mu\text{m}^2$ images of the surface at various stages of SAM growth was collected. Prior to immersion, the flame-annealed Au surface is very flat (Figure 3, 0 min). At 3 min, there are small bumplike features that are $\sim 20 \text{ nm}$ in diameter and randomly scattered over the surface. These stationary bumps are the smallest islands observed. Their actual size is not possible to determine and the observed $\sim 20\text{-nm}$ diameter is simply the radius of the AFM tip. At 6 min (not shown), we observe an increase in the density of these “seed” islands, and at 10 min, larger island assemblies begin to grow from these seed islands. The islands continue to grow and begin to touch one another (40 min). At 60 min, the growth is characterized by filling in the voids in and between the islands, a slow process which eventually leads to a complete SAM (5760 min).

From analysis of the images, we can determine the average island coverage of the surface, and the average island height, versus the immersion time, t (Figure 4). The island coverage (solid points, right scale) versus time shows three distinct stages of SAM growth. The initial nucleation phase, $0 \text{ min} < t < 8 \text{ min}$, is dominated by the formation of seed islands. These seed islands cover less than 10% of the surface before the next stage, $8 \text{ min} < t < 80 \text{ min}$, where island growth dominates. During the island growth phase, most of the surface becomes covered. The final coalescence stage is described by filling voids, and by far most of the growth time is spent to complete the final 20% of SAM coverage.

Average island height plotted versus the immersion time is also measured (Figure 4, open points, left scale). We clearly see that the island height peaks during the island

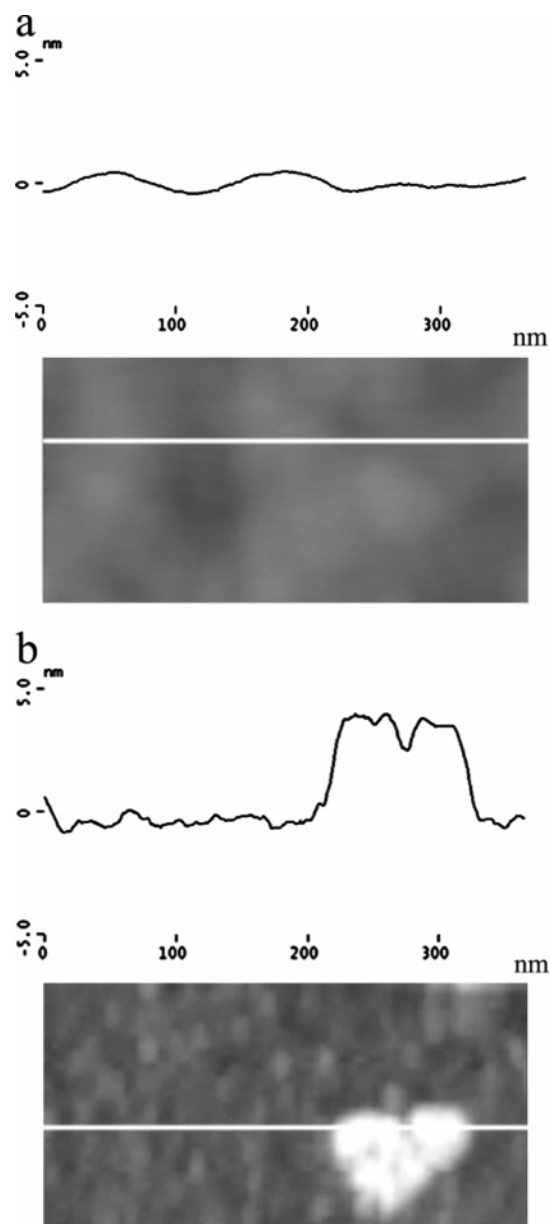


Figure 5. Details of two AFM images ($330 \times 190 \text{ nm}^2$) showing (a) flame-annealed Au and (b) a PEG island after 10-min immersion time. (b) Shows both the random background of laying down PEG (left side) and the higher island PEG (right side). The flame-annealed Au surface has a different variation in height than the random background of laying down PEG. The island height is defined as the distance from a low point of the laying down PEG close to the island to the flat plateau at the top of the nucleated PEG.

growth phase. This observation suggests that island growth is also associated with a rearrangement of the PEG molecules within the island, as discussed below.

The high contrast of the AFM for changes in surface height allow one to clearly distinguish the islands from the background; however, the limited lateral resolution inhibits our ability to see the exact molecular detail of the island. To compare the flame-annealed Au background (Figure 5a) with the partially formed SAM (Figure 5b), we examine two line scans of such surfaces, respectively. We clearly see the island feature with height 4.2 nm from the background (Figure 5b). The dip at the top of the island is due to a void in the island, which probably goes to the bottom of the island, but cannot be resolved because of the finite radius of the AFM tip. A comparison of the

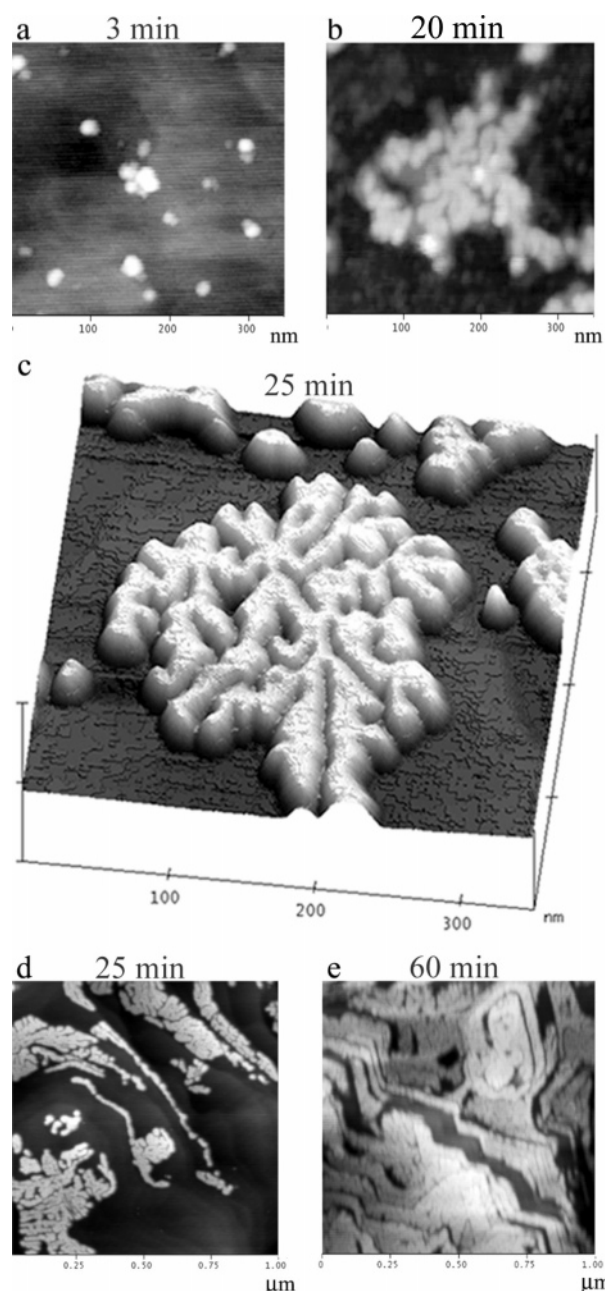


Figure 6. Detailed study of different features of the PEG SAM. (a) 3-min immersion time: The nucleation phase consisting of seed islands. The islands are made up of one or a few small bumps. (b) 20-min immersion time: Early stage island showing the bump structurelike features. (c) 25-min immersion time: Dendrites of PEG SAM with a branching structure and many voids. (d) 25-min immersion time: Growth along terrace steps in the Au surface. (e) 60-min immersion time: The Au(111) sixfold symmetry effecting the SAM structure. The height scale is 15 nm for all images.

background features shows that the partially assembled SAM has background fluctuations on a much shorter length scale than the clean Au (Figure 5a and lower region of 5b).

A study of the fine structure also reveals several details of the morphology of the PEG SAM. The nucleation stage of the PEG SAM consists of single or small groups of small bumps (Figure 6 a). These bumps appear to make up the structure of the small islands (Figure 6b). The dendritic character of the larger islands is clearly seen at later times in the SAM formation (Figure 6c and d). The island growth is also influenced by the terrace steps in the Au, and islands

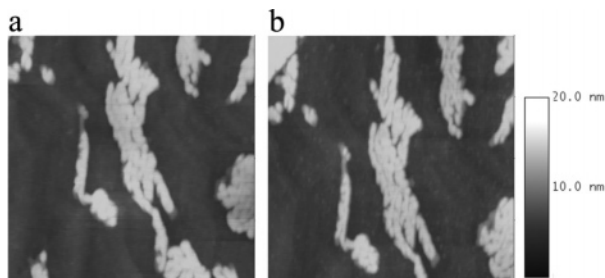


Figure 7. Comparison of AFM images of the same area in an (a) ethanol and a (b) PBS environment. The island morphology and height is not effected by the change of solvent within the resolution of the microscope.

are seen to grow along such steps (Figure 6d). On a large scale, the sixfold symmetry of Au(111) surface is clearly visible in the partially completed PEG SAM (Figure 6e).

To determine the effect of the solvent of an already partially assembled PEG SAM, we make a comparison by imaging the same area, both in ethanol and PBS with pH 7.4 (Figure 7). This experiment demonstrates how the morphology and the island height of the PEG is unaffected by the change between these two solvents within the resolution of the AFM. Conclusions drawn from the PBS case can be extrapolated to ethanol. The advantage of imaging in PBS is the physiological environment, but also the practicality of using a fluid which forms a good droplet and does not rapidly evaporate.

Discussion

Mechanisms for SAM Formation. The simplest description of the dynamics of monolayer formation is the Langmuir model which predicts an exponential time dependence of surface coverage.¹⁴ The Langmuir model is based on a mean field assumption (that the rate increase of coverage is proportional to the average amount of free surface) and it applies to noninteracting molecules randomly sticking to a surface. Such a model will not give island growth as observed in these experiments (Figures 3 and 6). However, attempts have been made to extend the Langmuir model to include island growth.¹⁷ Island growth arises when an attractive interaction between molecules is present, with the consequence that the probability of sticking becomes proportional to the local configuration of molecules. Therefore, one general finding from our experiments is that attractive interactions exist between the PEG molecules in ethanol. Whether this is a consequence of attraction originating from intermolecular hydrogen binding between amide groups^{8,18} or a fundamental property of a PEG SAM cannot be determined by these data.

We believe that models of island growth based on diffusion-limited aggregation (DLA)^{19,20} are particularly relevant to the dendritic growth observed for the PEG SAM (Figure 6b, c, d and Figure 7), as well as for the dendritic features which have been reported for an octadecyltrichlorosilane-based monolayer on oxidized Si(100).²¹ In the DLA models, molecules randomly attach to the surface and then diffuse on the surface by hopping

between atomic sites. An attractive interaction between the diffusing molecules results in the nucleation of small, stable seed islands, which stop diffusing as they reach a critical size. These stable islands then grow as the SAM starts to cover the surface. The growing islands eventually begin to touch one another and the completion of the SAM is the coalescence of these islands, where a rather long time may be required to fill all voids and vacancies within and between islands. This three-stage growth process, nucleation, island growth, and island coalescence, is observed in growth of molecular layers on surfaces where attractive interactions between molecules exist.²² An important parameter influencing the growth in such models is the dimensionless ratio of the surface diffusion constant, D , to the rate of attachment from solution, F , $R = D/F$. When R is large, the surface will have a low density of seed islands, and the growing islands will have a dendritic form, with multiple branches and many voids and vacancies. When R is small, seed islands are formed with higher density, and growing islands touch one another before large dendritic islands are formed.

The island coverage of our PEG SAM growth follows these three distinct stages, each with a characteristic growth rate. A linear fit of island coverage versus immersion time in each of the three gives island growth rates of 0.90, 1.34, and 0.00256% surface island coverage/min, respectively. This measurement shows that island growth is approximately a factor 1.5 faster than island nucleation. In the coalescence stage, the growth rate is about a hundred times slower than the initial stages. When comparing the three different growth stages (Figure 4, solid points, right scale) with the number and appearance of the islands (Figure 3), the data is consistent with the three-stage growth predicted by the DLA model.

A hallmark feature of a DLA growth scenario is the formation of dendritic island structures. The appearance of such islands might well be explained by surface diffusion being the dominate factor in island growth. Models of DLA predict that the fractal dimension of the islands should be in the range 1.5–1.7, depending on the coordination of the underlaying lattice and the anisotropy of the growth.²³ We are not able to extract a reliable measure of the fractal dimension of our islands because of AFM tip convolution effects, which hide the detailed features of the island at the single molecule scale. We observe highly dendritic islands when growth occurs on a particularly flat area (Figure 6c). However, more frequently islands appear to be bounded by steps in the Au surface (Figure 6d, e). The influence of these steps on the island growth makes a quantitative comparison with theoretical predictions about island growth difficult in our experiments. Various theories give asymptotic predictions about the statistical distribution of island size,^{19,24} but experimental determination of such quantities would require data accumulated over many, large flat areas without atomic steps influencing the growth.

DLA has been widely used to describe the growth of atomic layers from vapor deposition on hot surfaces (molecular beam epitaxy), a situation for which the model seems well suited. However, the extension of this model to the growth of polymer SAMs in solution is not entirely obvious. The long tail of the polymer attached to the surface (~ 13 Au lattice sites for our molecule) will move randomly in the solute and presumably has some influence on the

(17) Dannenberger, O.; Buck, M.; Grunze, M. *J. Phys. Chem.* **1999**, *103*, 2202–2213.

(18) Clegg, R. S.; Reed, S. M.; Hutchison, J. E. *J. Am. Chem. Soc.* **1998**, *120*, 2486–2487.

(19) Amar, J. G.; Family, F. *Phys. Rev. Lett.* **1995**, *74*, 11, 2066–2069.

(20) Amar, J. G.; Family, F. *Phys. Rev. B* **1994**, *50*, 12, 8781–8797.

(21) Carraro, C.; Yauw, O. W.; Sung, M. M.; Maboudian, R. *J. Phys. Chem. B* **1998**, *102*, 4441–4445.

(22) Himmelhaus, M.; Eisert, F.; Buck, M.; Grunze, M. *J. Phys. Chem.* **2000**, *104*, 576–584.

(23) Popescu, M. M.; Hentschel, H. G. E.; Family, F. *Phys. Rev. E* **2004**, *69*, 061403.

(24) Doudevski, I.; Schwartz, D. K. *Phys. Rev. B* **1999**, *60*, 1, 14–17.

binding of other molecules over an area which is significantly larger than an atomic scale object. However, DLA is to our knowledge the only mechanism resulting in dendritic island growth. Furthermore, SAM growth by surface diffusion has also been observed in AFM studies for an alkane thiol system.^{25–27}

Although the islands at later immersion times have a dendritic structure, the initial nucleation of an island appears to have a form similar to that reported for other SAM systems.²⁸ The nuclei are likely composed of a small aggregate of PEG molecules (Figure 6a). However, the size of these structures is close to that expected for the tip radius of curvature ~ 20 nm, and therefore we cannot determine if the nuclei contain only one or as many as a hundred molecules. Often, we find that these nuclei have a “double bump” form, indicating that there is some internal structure to the seed islands. Because of their random orientation, these structures cannot be artifacts from the AFM tip geometry. We have also observed that these nuclear islands tend to congregate on the surface, acting as building blocks for larger islands (Figure 6b). Such behavior is, however, not universally observed, and it is difficult to draw any strong conclusions from these observations.

Molecular Conformations of the PEG SAM. The conformations of the molecules in a PEG SAM have been much more studied than the morphology and dynamics of SAM growth. The PEG molecule conformations in a SAM are effected by many different factors, such as solvent,⁷ temperature,²⁹ substrate-headgroup binding,⁹ number of ethylene glycol (EG) units,^{6,8} and the energies of different molecular conformations because of intra- and intermolecular interactions.³⁰ These factors determine the two most commonly observed phases of OEG and PEG: a disordered melt phase and a highly ordered crystalline phase.^{6–10,16} Coexistence of the two phases is also possible where, locally on the surface, one or the other phase is dominant. The different phases of PEG originate in the EG molecule, the subunit of PEG. EG consists of two methylenes and an oxygen atom which can achieve different rotational configurations, resulting in an ordered or disordered SAM.

The molten phase describes a wide distribution of rotational conformations (also called gauche rich), a strongly disordered state of the polymer. Characteristic for the molten phase is molecules laying down parallel to the surface plane rather than being oriented toward the surface normal, which is the case for the crystalline phase. The molten phase of PEG has its analogue in the laying down phase of the alkane thiol, which is the alkane chain conformation in early island formation.^{25,31} A few of our detailed studies reveal background fluctuations in the areas not occupied by PEG islands. (Figure 5 and Figure 6b). The nature of these fluctuations is, with the case for alkane thiols in mind, due to a dilute layer of diffusing PEG molecules on the surface, with their tails oriented parallel to the surface. The laying down molecules are not yet incorporated in the island structure but as the island

grows the laying down molecules change to crystalline phase as they are added to an island. We have also performed infrared reflection absorption spectroscopy (IRAS) measurements which show that the average phase of the PEG SAM is moving toward a crystalline state with increasing immersion time, supporting this picture.¹⁶

The crystalline phase is described as a well-ordered state of the PEG moieties of the SAM. Two major conformations have been reported here, all-trans and helical.^{6,8} PEG in its most extended configuration is the all-trans zigzag structure. The more complicated helical structure is obtained by a rotation of the $\text{CH}_2\text{—OH}$ groups around the C—C axis. An intramolecular hydrogen bond makes a C—C gauche configuration energetically favorable³² resulting in a trans-gauche-trans conformational sequence of the three EG bonds O— CH_2 , C—C, and O— CH_2 , respectively. Such a helical conformation contains seven structural units of $\text{CH}_2\text{—CH}_2\text{—O}$ with two helical turns (7/2 helix) with the length of 19.3 Å. (For comparison, the length for seven units of the all-trans conformation is 23.9 Å.)¹⁰ This helical conformation is believed to be favorable over the molten state in an aqueous solution since the origin of the gauche effect observed in PEG and OEG is not an intrinsic property of the EG unit, but a result of the influence of a polar environment. This influence manifests itself even in an isolated OEG chain, where the trans-gauche-trans conformation of an EG unit is stabilized by the electric field created by its neighboring EG units. Further stabilization occurs in the alkanethiol SAM because of electrostatic interactions between neighboring chains.³³

For OEG-terminated alkane thiols, the conformation in the crystalline phase also has a dependence on the number of EG units and the temperature. Conformations obtained by a tetra(ethylene glycol) and a hexa(ethylene glycol) SAM at room temperature are all-trans and helical, respectively.²⁹ By gradually increasing the temperature, the helical structure undergoes a transition to an all-trans conformation. The tetra(ethylene glycol) is marginally affected by raising the temperature, with a slight increase of disorder in the PEG moiety.

The conformation of a thiol PEG can also be related to the substrate properties. The sulfur atoms of an alkane thiol SAM on Au(111) are arranged in a hexagonal lattice with 4.97 Å and an idealized packing density of 21.4 Å²/thiolate.³⁴ Crystalline PEG in its helical form has a molecular cross section of 21.3 Å². The lateral constraints in the densely packed phase with helical thiol OEG moieties adopt an orientation parallel to the surface normal and attain their bulk mass density. The cross section of the all-trans conformation is 17.1 Å² with an idealized packing density of 19.1 Å²/thiolate.³⁴ The influence of the substrate on the PEG conformation was demonstrated in a study of the same PEG thiol assembled onto Au and Ag.⁹ The larger lateral spacing between the atoms of Au over Ag allows for the helical structure conformation (trans-gauche-trans) of the PEG to form, whereas on Ag, where the lateral spacing is smaller, an all-trans PEG is formed. Because of lateral constraints in the densely packed crystalline structure of both crystalline states, the OEG moieties adopt an orientation parallel to the surface normal and attain their bulk mass density.

One surprising finding in our data is that the height of the islands formed during island growth first climbs from

(25) Xu, S.; Cruchon-Dupeyrat, S. J. N.; Garno, J. C.; Lui, G.-Y.; Jennings, G. K.; Yong, T.-H.; Laibinis, P. E. *J. Chem. Phys.* **1998**, *108*, 12, 5002–5012.

(26) Poirier, G. E.; Pylant, E. D. *Science* **1996**, *272*, 1145–1148.

(27) Camillone, N., III. *Langmuir* **2004**, *20*, 1199–1206.

(28) Doudevski, I.; Hayes, W. A.; Schwartz, D. K. *Phys. Rev. Lett.* **1998**, *81* (22), 4927–4930.

(29) Valiokas, R.; Östblom, M.; Svedhem, S.; Svensson, S. C. T.; Liedberg, B. *J. Phys. Chem. B* **2000**, *104*, 7565–7569.

(30) Gejji, S.; Tegenfeldt, J.; Lindgren, J. *Chem. Phys. Lett.* **1994**, *226*, 427–432.

(31) Yamada, R.; Uosaki, K. *Langmuir* **1998**, *14*, 855–861.

(32) Crupi, V.; Janelli, M. P.; Magazù, S.; Maisano, G.; Majolino, D.; Migliardo, P.; Sirna, D. *Mol. Phys.* **1985**, *84*, 4, 645–652.

(33) Pertsin, A. J.; Grunze, M.; Garbuzova, I. A. *J. Phys. Chem. B* **1998**, *102*, 4918–4926.

(34) Dubois, L. H.; Zegarski, B. R.; Nuzzo, R. G. *J. Chem. Phys.* **1993**, *98*, 678–688.

3 nm (1-min immersion time) at the nuclei step to ~ 5 nm for the small islands (25-min immersion time) and then falls gradually to 3.5 nm (60-min immersion time and higher) as the fractional coverage increases (Figure 4, open points, left scale). We interpret the change in island thickness in the light of the different conformations for the PEG moiety in an alkane thiol PEG SAM discussed above. Common for all the above-mentioned studies of PEG SAMs is the lack of dynamical data. All analysis was done on a SAM which is considered complete and is analyzed when the assembly process is finished and any conformational changes during SAM formation would be undetected.

Thus, it is tempting to speculate that the height change seen here reflects conformational changes in the PEG from all-trans to helical, which would suggest that PEG conformations are dependent on lateral surface density in some unusual way. The predicted height difference between the two conformations of all-trans and helical for our 17-unit PEG is 1.1 nm, which is also the measured height difference from the peak at 20-min immersion time to the plateau at 60 min and longer immersion time (Figure 4, open points, left scale). This observation supports the assumption of a conformational transition. However, in the all-trans conformation, the molecule used has a predicted length of 5.8 and 4.7 nm in the helical conformation, which is longer than the measured thicknesses. We do not believe that this difference in predicted and measured height has its origin in a molecular tilt because of the dense packing of PEGs on Au as discussed above. One possible contribution to this difference is that the lower point in the island height measurements is not the Au surface but rather the top of a layer of laying down PEG surrounding the island. Another issue is the solution dependence of the PEG which has been reported for the crystalline phase for the PEG moiety in a SAM where the top section of the PEG is disordered, while the majority of the molecule is in an ordered state in an aqueous solution.⁷ This disorganized top part of the PEG is also consistent with contact angle goniometry measurements on a similar SAM where the surface shows a hysteretic behavior with $\sim 6^\circ$.¹⁶ The result of such unstable PEG should be a rearrangement of the top layer of the PEG SAM when in contact with the scanning AFM probe and a decrease in the appearance of the island height. To understand the full picture of the island height change, several techniques, spectroscopic as well as AFM, should be used in parallel in a time-lapse experiment.

Implications for Building PEG Based Surfaces.

We have noticed that the SAM system is easily disturbed and that several attempts to make a SAM failed so that even after immersion times over several days a monolayer did not form on the surface. The failures were probably

due to surface contamination, and the yield was improved by carefully boiling the Au surface and the tweezers with TL1 solution and by using clean Nalogene beakers (VWR International) washed with ethanol in ultrasound. To avoid any sources of error and contamination, we always handle the chip with the clean tweezers and make sure that the only thing in contact with the sample during AFM imaging is the fluid cell, which is carefully washed with soap solution.

Extensive attempts to perform a SAM growth study in situ, to observe molecules binding to the surface while scanning with the AFM, have been unsuccessful. We believe that this lack of success is due to contamination in the experimental setup which, despite careful cleaning of the components of the setup, disturbs the sensitive monolayer formation.

Conclusions

This AFM study of the SAM formed by the amide-containing poly(ethylene glycol) (PEG) thiol ($\text{CH}_3\text{O}-(\text{CH}_2\text{O})_{17}\text{NHCO}(\text{CH}_2)_2\text{SH}$) has shown dendritic island formation. The island surface coverage follows three distinct steps with different growth rates: island nucleation, growth, and coalescence, where the last step is significantly slower than the first two. This three-step growth is consistent with computer simulations of DLA growth. We have also observed a change in the island height, which peaks during the island growth phase. This height change can be associated with a molecular conformational transition within the crystalline phase. A disordered phase of the PEG is seen surrounding the island formations, which probably consists of molecules laying down on the surface. This state is associated with the molten phase of the PEG.

Acknowledgment. The authors thank the Swedish Research Council (VR) for funding. We also acknowledge Anders Wirsén at the Department for Polymer Technology at the Royal Institute of Technology in Stockholm for contributing with his expertise on polymers and SAMs and Ramunas Valiokas and Bo Liedberg at the Department of Physics and Measurement Technology at the Linköping University for showing us how to make good SAMs.

Note Added after Post-ASAP Publication. There was an error in the PEG formula that appears in the abstract and the third paragraph of the Experimental Section in the version published ASAP February 17, 2005; the corrected version was published ASAP March 16, 2005.

LA0471792